Digest Journal of Nanomaterials and Biostructures Vol. 9, No. 3, July - September 2014, p. 929 - 934

pH SENSING USING GROWTH OF INN NANORODS ON GLASS SUBSTRATES

S.P. CHANG, S. WANG
Institute of Microelectronics & Department of Electrical Engineering, Center for Micro/Nano Science and Technology, Advanced Optoelectronic Technology Center, National Cheng Kung University, Tainan 70101, Taiwan

In this work, the sensing cell of pH sensors with an vertically aligned InN nanorods array with a uniform diameter and length was fabricated on a glass substrate by plasma-assisted molecular beam epitaxy. The nanorod diameters were measured to be between 60 and 150 nm and have a length of around 500 nm.The InN nanorods with high crystalline quality grow preferentially in the (0002) direction over a large area. The resulting pH sensors with InN nanorods exhibited significantly improved sensing performances owing to the large sensing surface-tovolume ratio. The pH sensitivity calculated from the linear relation between the cyclic voltammetry current and the pH value was 5.4 nA/pH.

(Received May 12, 2014; Accepted July 4, 2014)

Keywords: InN, Nanorod, pH Sensor, Molecular Beam Epitaxy, Heteroepitaxy

1. Introduction

The distinctive properties of InN, such as the high absorp- tion coefficient, high carrier mobility, large drift velocity, and a narrow direct band gap about 0.8ev, make the use of InN and related alloys for solar energy harvesting and near- infrared-optoelectronic applications an attractive proposition. InN nanorod surfaces respond electrically to variations of the pH in electrolyte solutions introduced via an integrated microchannel [1]. The ion-induced changes in surface potential are readily measured as a change in conductance of the InN nanorods and suggest that these structures are very promising for a wide variety of sensor applications [2-6]. However, the development of the III-nitride-semiconductor solar-harvesting market is always impeded by the size and cost limitations of the fabrication. The main challenge in cell fabrication is achieving a reasonable material quality on a low-cost, large-area substrate. Thus, forming InN nanorods on low-cost glass substrates by heteroepitaxy could be an alternative way of developing high-performance cells. We report here on the epitaxial growth of InN nanorods on AlN/glass template. An InN/AlN heterojunction structure has been noted to provide a possible platform for future InN-based device applications due to its potentially excellent structural and electronic properties as a consequence of the large band gap difference between InN and AlN. This provides naturally formed nucleation sites for the subsequent directional growth of InN nanorods along the c-axis. In this letter, InN nanorod pH sensors were successfully fabricated by plasma-assisted molecular beam epitaxy on a glass substrate. Properties of the fabricated pH sensor will also be discussed.

2. Experimental

The InN nanorods were grown by plasma-assisted molecular beam epitaxy (PAMBE) on quartz glass. The PAMBE system was equipped with an RF plasma source providing active nitrogen

* Corresponding author: changsp@mail.ncku.edu.tw

and with standard K-cells for In and Al. A 7N pure In metal source was loaded into a K-cell, and the 6N pure nitrogen gas source was further purified by a nitrogen purifier and fed into the RF plasma generator. Prior to growth, the substrate was cleaned ultrasonically with acetone, ethanol, and deionized water sequentially. An 80-nm-thick AlN buffer layer was first deposited onto the substrate at a temperature of 890 °C. The substrate temperature was then cooled to 450 °C to grow the InN nanorods under In-rich regime. The growth was performed by exposing the glass substrates to an N_2 flux of 1.2 sccm for 4 hr at an RF plasma power density of 12 mW/cm^3 and background pressure of 10^{-9} Torr. To measure the sensing performances of the fabricated pH sensors, the pH sensor and the Ag/AgCl reference electrode were dipped into the detection solution (pH value varied from 5 to 11). The pH value of the buffer solution was varied from 5 to 11, and the pH value which was depend on the concentration of the H^+ ions. In order to achieve our demands, we used the hydrochloric acid and the sodium hydroxide to mix the pH value which we expected. As shown in Fig. 1, the sensing response of the pH sensors was measured using an CH Instrument Model 600D analyzer.

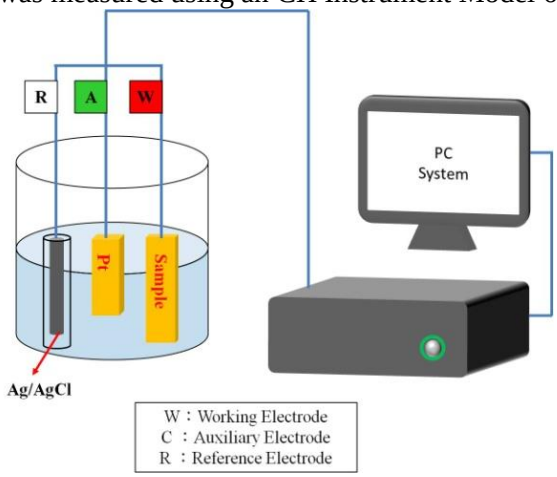

Fig. 1 Schematic diagram of electro-chromic system

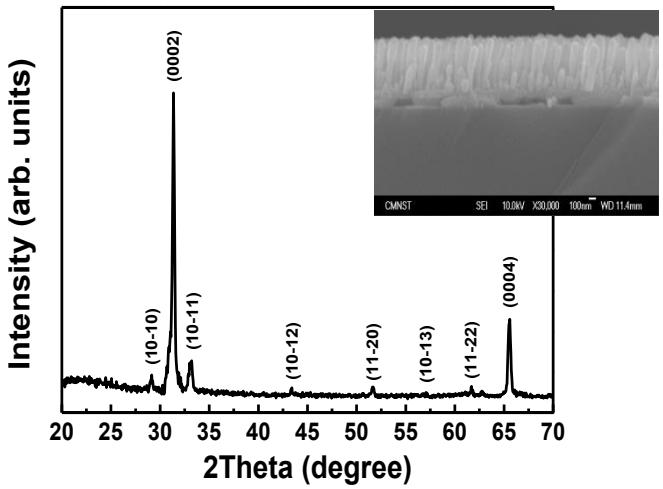

Fig. 2 X-ray diffraction of the InN nanorods on the glass substrate. The inset shows cross-sectional FESEM images of vertically aligned InN nanorods on a glass substrate.

3. Results and discussion

The morphology and size distribution of the InN nanorods were characterized by a field-emission scanning electron microscope (FESEM) operated at 10 keV. As shown in the inset of Fig. 2, the cross-sectional view shows high density vertical InN nanorods with uniform diameter and

uniform length were grown on the glass substrate. The nanorod diameters were measured to be 100 nm on average with a length of around 500 nm. The nanorod ensembles with a high aspect ratio and large surface-to-volume ratio are hexagonal in shape, which is probably due to the wurtzite structure of the InN crystal. Figure 2 shows wide-angle 2θ–ω X-ray diffraction (XRD) profile of Nthe InN nanorods. The main peaks can be identified as InN (0002) and InN (0004), which is consistent with the c-axis orientation structure of rods in SEM image. Other peaks are attributed to InN (10-11), InN (10-12), and InN (10-13), which are reflections from the sloped sides of the nanorod's tip. The InN (10-10) peak is likely to originate from a small percentage of uprooted rods laying parallel to the substrate.

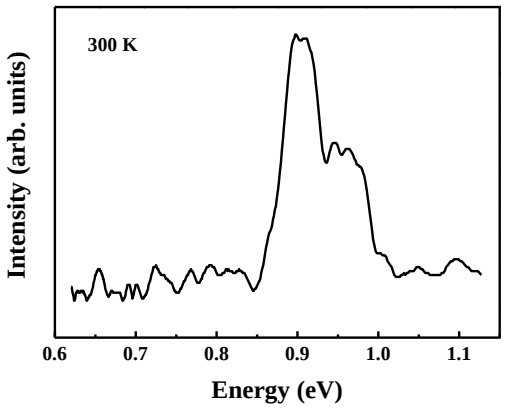

Fig.3. PL spectrom of the InN ranorods on a glass substrate.

Fig. 3 shows the PL spectrum of the InN nanorods measured at room temperature. The spectrum shows the band edge luminescence of 0.89 eV with the full width at half maximum (FWHM) of 0.10 eV. This PL peak energy is in agreement with the reported value [7] for InN nanorods with diameter of ~100 nm. However, the PL bands observed from nanorod samples show slight blueshift and broadened bandwidth compared with the InN films. [8] It is presumed that the blueshift could be attributed to the high carrier concentration with the conduction band being significantly filled because of the limited density of states.

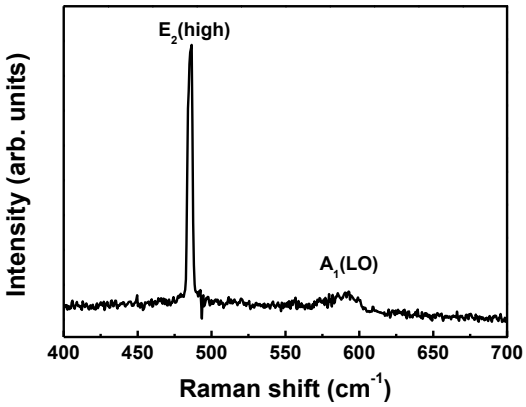

Fig. 4. Room-temperature Raman spectrum of the InN nanorods on the glass substrate.

The room-temperature Raman spectrum in Fig. 4 shows two active optical phonons that can be assigned to an InN A_1 longitudinal optical (LO) phonon at ~591 cm^{-1} and an E_2 (high) phonon at ~486 cm^{-1}. According to the selection rules, in a Raman geometry configuration of $z(x,x)z^-$, the A_1 (LO) and E_2 (high) phonons are activated for hexagonal crystalline InN, i.e., the presence of these modes confirms the wurtzite structure [9]. It should be mentioned that the Raman scattering peak at ~449 cm^{-1} due to the A_1 transverse optical (TO) phonon mode was not observed. The absence of this

mode is consistent with good crystalline quality of the nanorods since a large disorder density or polycrystalline structure would excite the A_1 (TO) mode [10]. However, the E_2 (high) mode seen here is redshifted in comparison to the standard values reported in the literature [11-13]. The E_2 modes correspond to atomic oscillations in the c-plane, and therefore, the mode frequency, especially that of the high-frequency mode, is sensitive to lattice strain in the c-plane. Perlin *et al.* [14] have reported the effects of pressure on the Raman spectra of GaN. The strain in the GaN layers can be thought as a superposition of a hydrostatic pressure and a biaxial pressure in the growth plane [15]. They found that the E_2 (high) modes were redshifted as the hydrostatic pressure was reduced. We believe InN would show similar behavior to GaN, and hence suggests that the hydrostatic strain is small but still exists in our InN nanorods. Furthermore, the presence of dislocations in the coalescence junctions, which provides a channel for the residual strain in the InN to relax [12], presumably generates a rather complex strain field.

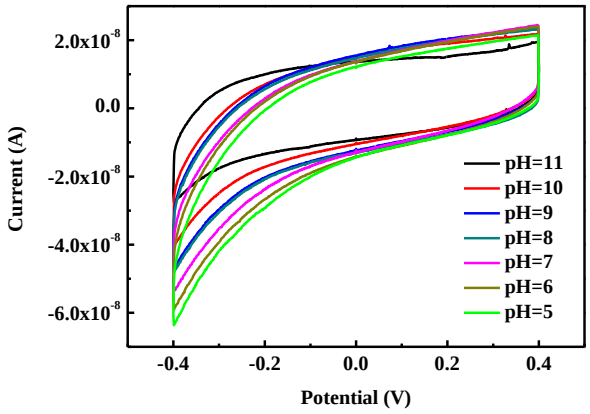

Fig. 5 Sensing current vs. reference potential characteristics of pH sensor with InN nanorods on the glass substrate.

Fig. 5 shows the cyclic voltammograms (CV) curves for the InN nanorod in the solutions from pH 5 to 11. Cyclic voltammograms were recorded in the potential range of −0.4 to 0.4V. In each pH solution, there were no obvious redox peaks of the InN nanorods was observed. Besides, the cathodic peak potentials shifted towards negative direction as the decrease of pH while the anode peak remains nearly constant at the value of $2x10^{-8}$A. Moreover, the pH sensitivity calculated from the linear relation between the sensing current and the pH value was 5.4 nA/pH. Fig. 6 depicts the pH dependence of the reference current at different bias voltage. InN nanorods array shows good respond to pH.The calibration curve corresponding to current response is nearly linear against the change of pH ranging from pH 5 to pH 11 . Comparing these three curves, the one biasing at 0V exhibited the best linearity .When the biasing voltage was declined, the pH sensitivity increased considerably. Nevertheless, the pH sensitivity deviated slightly from linearity as shown in Fig 6. This result shows that the shift of the biasing voltage severely altered the response of the current. So the conclusion could be obtained that the increase of the magnitude of biasing voltage raised the electron mobility and the current.

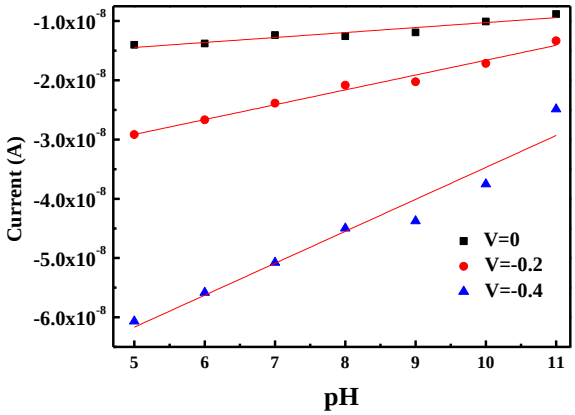

Fig. 6 Reference current as a function of pH value at different bias.

4. Conclusions

In conclusion, InN nanorod pH sensors were successfully fabricated by plasma-assisted molecular beam epitaxy on low-cost glass substrates. It was found that the average length and average diameter of the nanorods were 500 nm and 100 nm, respectively. The experimental results indicate that the nanorod sensor is a useful and successful structure. Therefore, InN nanorod sensors indeed can be applied in pH sensing and demonstrate good performance.

Acknowledgments

The authors thank the National Science Council and Bureau of Energy, Ministry of Economic Affairs of Taiwan, R.O.C., for the financial support under Contract No. 101-2221-E-006-139 and 102-E0603, and the LED Lighting Research Center of NCKU for the assistance with device characterization. This work was also supported in part by the Center for Frontier Materials and Micro/Nano Science and Technology, the National Cheng Kung University, Taiwan, as well as by the Advanced Optoelectronic Technology Center, the National Cheng Kung University, under projects from the Ministry of Education.

References

[1] K. H. Lee, S. P. Chang , K. W. Liu, P. C. Chang, S. J. Chang, T. P. Chen, H. W. Shiu, L. Y. Chang, C. H. Chen, Sci. Adv. Mater. **5**, 873 (2013)
[2] F. Werner, F. Limbach, M. Carsten, C. Denker, Nano Lett. **9**, 1567 (2009)
[3] K. H. Lee, S. P. Chang, K. W. Liu, P. C. Chang, S. J. Chang, T. P. Chen, H. W. Shiu, L. Y. Chang, and C. H. Chen, Int. J. Electrochem. Sci. **8**, 3212 (2013)
[4] H. Lu, W. J. Schaff, and L. F. Eastman, J. Appl. Phys. **96**, 3577 (2004)
[5] C. F. Chen, C. L. Wu, and S. Gwo, Appl. Phys. Lett. **89**, 252109 (2006)
[6] Y. S. Lu, C. L. Ho, J. A.Yeh, H. W. Lin, and S. Gwo, Appl. Phys. Lett. **92**, 212102 (2008)
[7] Z. Liliental-Weber, X. Li, O. Kryliouk, H. J. Park, J. Mangum, and T. Anderson, AIP Conf. Proc. **893**, 111 (2007)
[8] H. Y. Chen, C. H. Shen, H. W. Lin, C. H. Chen, C.-Y. Wu, S. Gwo, V. Y. Davydov, A. A. Klochikhin, Thin Solid Films **515**, 961 (2006).
[9] V. Yu. Davydov, V. V. Emtsev, I. N. Goncharuk, A. N. Smirnov, V. D. Petrikov, V. V. Mamutin, V. A. Vekshin, S. V. Ivanov, M. B. Smirnov, and T. Inushima, Appl. Phys. Lett. **75**, 3297 (1999).
[10] X. H. Ji, S. P. Lau, H. Y. Yang, and Q. Y. Zhang, Thin Solid Films **515**, 4619 (2007).

[11] O. Kryliouk, H. J. Park, Y. S. Won, T. Anderson, A. Davydov, I. Levin, J. H. Kim, J. A. Freitas, Nanotechnology **18**, 135606 (2007).
[12] J. W. Chen, Y. F. Chen, H. Lu, and W. J. Schaff, Appl. Phys. Lett. **87**, 041907 (2005).
[13] Z. H. Lan, W. M. Wang, C. L. Sun, S. C. Shi, C. W. Hsu, T. T. Chen, K. H. Chen, C. C. Chen, Y. F. Chen, L. C. Chen, J. Cryst. Growth **269**, 87 (2004).
[14] P. Perlin, C. Jauberthie-Carillon, J. P. Itie, A. S. Miguel, I. Grzegory, and A. Polian, Phys. Rev. B **45**, 83 (1992).
[15] R. F. Davis, S. Einfeldt, E. A. Preble, A. M. Roskowski, Z. J. Reitmeier, and P. Q. Miraglia, Acta. Mater. A **51**, 5961 (2003).